3rd Brazil-France Symposium on Medicinal Chemistry
Maceió/AL | November 12 -14, 2024

# MOLECULAR MODELING PROPOSES *Schistosoma mansoni* CATHEPSIN-B1 (*Sm*CB1) INHIBITION BY SPIRO-ACRIDINE DERIVATIVES

**Fernanda de França Genuíno Ramos Campos (G)[1,3]*, Arthur Gabriel Corrêa de Farias (G)[1,3], Igor José dos Santos Nascimento (Prof)[1,2], Ricardo Olímpio de Moura (Prof)[1,2,3].**

ffgrcampos@gmail.com;

[1]*Drug Development and Synthesis Laboratory, State University of Paraíba, Paraíba, Brazil.*
[2]*Postgraduate Program in Pharmaceutical Sciences, State University of Paraíba, Paraíba, Brazil.*
[3]*Pharmacy Department, Center for Biological and Health Sciences, State University of Paraíba, Paraíba, Brazil.*

*Keywords: schistosomiasis, spiro-acridines, molecular docking, density functional theory.*

## ABSTRACT

**INTRODUCTION:** Infection by *Schistosoma mansoni* is a great burden on developing countries, while current treatments find themselves outdated as organisms develop increasing resistance. Recent evidence indicates that enzyme Cathepsin B1 (*Sm*CB1) is a critical part of this parasite's growth, as when it is inhibited, *S. mansoni* perishes at any of its life cycle stages, due to impaired nutrient digestion. Derivatives of (E)-1'-(benzylideneamino)-5'-oxo-1',5'-dihydro-10H-spiro[acridine-9,2'-pyrrole]-4'-carbonitrile (AMTAC-01) were previously reported to exhibit antiparasitic activity by inhibiting critical enzymes in other organisms, suggesting also a potential role in *Sm*CB1 inhibition.

**OBJECTIVE:** In order to identify potential new antischistosomal drugs, 22 spiro-acridine derivatives (AMTAC-series) were evaluated for their potential *Sm*CB1 inhibition through virtual screening based in non-covalent docking, covalent docking and density functional theory (DFT).

**METHODS:** Docking of the known inhibitor (ORW) in *Sm*CB1's active site before covalent binding was performed (PDB ID: 6YI7) with AutoDock Vina and UCSF Chimera, employing a cubic grid box of 20 Å in all axes, centered in XYZ coordinates -20, 10 and -22 Å respectively. Pre-binding ORW was drawn, conformationally analyzed and geometrically minimized (PM3) through Avogadro and ORCA, as well as all 22 AMTACs. The highest-scored pose, where a lesser than 6 Å distance between $Cys^{100}$ and its' nitrile group was maintained, was subsequently used for non-covalent docking in GOLD. A distance restriction of 1,5-6,0 Å was imposed, while residues $Cys^{100}$ and $His^{270}$ were set as flexible, and method validation was obtained (RMSD = 1.685 Å). Only AMTAC compounds that surpassed ORW's fitness score (45.45) and maintained ≤ 6 Å distance between their nitrile groups and $Cys^{100}$ were accepted for covalent docking, also performed in GOLD and successfully validated (RMSD = 1.264 Å). Similarly, AMTACs were only considered promising leads if they surpassed ORW (78.61) and were not found to sterically collide with amino acid residues. DFT calculations for successful compounds were performed in ORCA, applying B3LYP/6-311G.

**RESULTS:** 5 derivatives managed to surpass non-covalent screening, however, only (E)-1'-((2,6-dichlorobenzylidene)amino)-5'-oxo-1',5'-dihydro-10H-spiro[acridine-9,2'-pyrrole]-4'-carbonitrile (AMTAC-10) was accepted after covalent docking, as all others displayed steric collisions (Fig 1A). Highest occupied (HOMO) and lowest unoccupied energy molecular orbital (LUMO) surface and energy gap analysis (Fig 1B) predicts higher reactivity for AMTAC-10's nitrile group, corroborated by its electron affinity (EA), suggesting possible covalent bonding to *Sm*CB1.

**CONCLUSION:** AMTAC-10 showed great *Sm*CB1 inhibition potential in molecular modeling studies. Further studies may confirm its predicted antischistosomal activity.

**Figure 1: (A)** Non-covalent and covalent docking results. **(B)** Frontier molecular orbital (FMO) surfaces, HOMO-LUMO energy gap ($\Delta E_{gap}$) and electron affinity (EA).

**(A)**

| LIGANDS | NON-COVALENT FITNESS SCORE | COVALENT FITNESS SCORE | STERIC COLLISIONS |
|---|---|---|---|
| ORW | 45.45 | 78.61 | None |
| **AMTAC-10** | **45.55** | **81.42** | **None** |
| AMTAC-12 | 53.78 | 81.54 | $Gly^{269}$ |
| AMTAC-17 | 46.29 | 86.47 | $Cys^{100}$ |
| AMTAC-18 | 46.50 | 87.14 | $Cys^{100}$ |
| AMTAC-21 | 58.75 | 78.82 | $Gln^{94}$ |

**(B)**

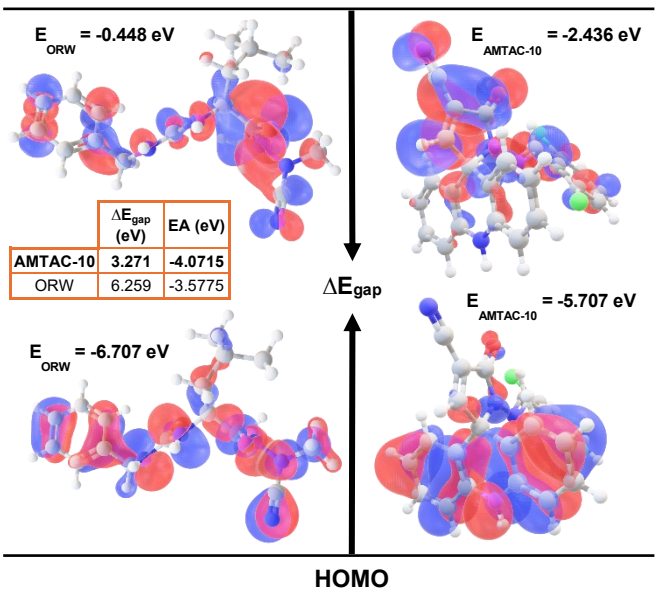


| | ΔEgap (eV) | EA (eV) |
|---|---|---|
| AMTAC-10 | 3.271 | -4.0715 |
| ORW | 6.259 | -3.5775 |